iJRASET
International Journal For Research in Applied Science and Engineering Technology

INTERNATIONAL JOURNAL FOR RESEARCH

IN APPLIED SCIENCE & ENGINEERING TECHNOLOGY

Volume: 10 **Issue:** VII **Month of publication:** July 2022

DOI: https://doi.org/10.22214/ijraset.2022.45227

www.ijraset.com

Call: 08813907089 | E-mail ID: ijraset@gmail.com

International Journal for Research in Applied Science & Engineering Technology (IJRASET)
ISSN: 2321-9653; IC Value: 45.98; SJ Impact Factor: 7.538
Volume 10 Issue VII July 2022- Available at www.ijraset.com

Retinal Analysis and Calculating Cup to Disc Ratio Value Using Deep Learning Models

Aashish Nayak[1], Dr. Dharamveer Singh[2], Vikas Gupta[3]
[1, 2, 3]*Deptt.of Computer Science & Engineering, R.D. Engineering College, Ghaziabad, India*

Abstract: ***Glaucoma is a disease of the retina caused by high intraocular pressure. The intraocular pressure in people with glaucoma can reach 60-70 mm Hg. This disease is characterized by an increasing cup to disc ratio size. Glaucoma has three levels, namely mild with a cup to disc ratio value of 0.3-0.5, moderate with a cup to disc ratio value of 0.5-0.7 and severe with a cup to disc ratio value above 0.7. For retinal analysis and calculating the cup to disc ratio value taken from a fundus camera, it must be done by an expert ophthalmologist, but it takes a long time. Therefore, feature detection and automatic cup to disc ratio value calculation are expected to assist doctors in analyzing glaucoma. The data used were 132 retinal fundus images consisting of 66 mild glaucoma images, 26 moderate glaucoma images and 40 severe glaucoma images taken from the RIM-ONE dataset (http://medimrg.webs.ull.es). Pre-processing techniques like cropping, resizing, brightness, Median Filter are used for noise removal. Subsequently, feature extraction with the help of GLCM. Consequently, the method used to classify the degree of glaucoma is the Deep Belief Network. The test simulation results obtained accuracy value of 99% with 99% of precision and 100% of recall.***

I. INTRODUCTION

A. Background

The development of vision systems has significantly simplified tasks in different areas of science in which activities such as machine learning, evolutionary computing, image processing, among others, are developed. In recent years, numerous vision systems have been developed that help solve problems in multiple real-life applications. Computer vision and image processing have a lot in common, the purpose of each being different. Image processing seeks to improve the quality of an image, such as eliminating defects, correcting blur, improving the quality of colors, among others. In which there is an input image and the improved image as an output. In the vision system the objective is to obtain the description and interpretation by computers, having an image as input, which will be processed to extract attributes and as output a description of the image. In the present work, a comparison and analysis of the performance of extraction and classification of characteristics in digital images that are obtained from patients with glaucoma and diabetic retinopathy are made, from which the most significant qualities of these are obtained, which are textural and chromatic characteristics. Glaucoma and diabetic retinopathy are eye diseases that affect vision causing total loss. For the first condition, the aqueous humor contained in the eye does not drain properly due to a failure of the ocular drainage system causing a higher intraocular pressure, this causes the nerve fibers that meet in the optic disc to be damaged and may die, preventing signals from reaching the optic nerve. Glaucoma is the second largest cause of blindness in the world (Bulletin of the WHO) and an estimated 80 million people will develop glaucoma by 2021 [1]. For retinopathy produced in diabetic patients, high sugar levels cause the blood vessels that feed the retina to die, the eye tries to create new of these structures to continue with the correct blood supply but these new vessels are weak which causes let them fracture and bleed. In the early stages of this condition, weak blood vessels dilate, generating lumps that protrude from the walls. The more blood vessels are damaged, the more serious it will be, because it causes the nerve fibers and the macula to become impawned. At this stage of the condition there is still treatment. The problem is aggravated, as already mentioned, with the death of the blood vessels, causing the detachment of the retina. Retinopathy can lead to glaucoma, as scar tissue affects the drainage of watery fluid. Automatic vision systems help efficient and effective detection without the intervention of a professional, speeding up the results. For them the importance of the best selection of textural and chromatic characteristics [2]. Glaucoma has been known for a long time, but not many people know about the dangers of this disease. If it is too late or not treated properly, glaucoma can cause permanent blindness in sufferers. Lack of awareness of the dangers of glaucoma is due to the symptoms of this disease that the glaucoma sufferer cannot feel directly [3]. Research to detect glaucoma has been carried out by several previous researchers, including research conducted by [4] who developed a glaucoma disease identification system through fundus images using the Backpropagation method which has a system accuracy rate of 98.45% [5] developed a system to detect glaucoma by combining Region of Interest (ROI) segmentation and

automated techniques system by using hemorrhage detection in certain areas of the fundus image with an regression rate of 86.17.57%. Another research was conducted by [6] who developed an automatic glaucoma detection system that was identified by calculating the cup to disc ratio (CDR). They have proven that if the CDR value is between 0.0-0.3 then the input image is normal. Meanwhile, if the CDR value obtained is greater than 0.3, the image is identified as glaucoma. This system has an F-score of 96%. Subsequent research conducted by [7] who developed a system for detecting glaucoma through optical disc and cup segmentation using K-mean clustering. The accuracy of the system they developed reached 92%. Based on the background and several studies using fundus images to identify glaucoma, the authors submitted a research proposal entitled "Identification of Glaucoma through Fundus Images Using a Deep Belief Network". The American Academy of Ophthalmology (2018) divides glaucoma into 3 types, namely open-angle glaucoma, closed-angle glaucoma, and glaucoma in children (childhood glaucoma). Open-angle glaucoma is further divided into primary open-angle glaucoma, normal-tension glaucoma, juvenile open-angle glaucoma, suspected glaucoma (glaucoma suspect), and secondary open-angle glaucoma. Angle closure glaucoma is also subdivided into primary angle - closure glaucoma with relative pupillary block, acute angle closure glaucoma, subacute angle closure glaucoma, chronic angle closure glaucoma, secondary closed angle glaucoma with and without pupillary block, and iris plateau syndrome. Primary open-angle glaucoma, the most common form of black and white races, causes an asymptomatic, progressive, bilateral visual field narrowing that arises slowly and often goes undetected until a broad narrowing of the field of view occurs. It is estimated that the prevalence of primary open-angle glaucoma in the United States in individuals over 40 years of age is 1.86% based on a population meta-analysis study (American Academy of Ophthalmology, 2018) [1-3]. Image is a representation (picture), similarity, or imitation of an object. Image is divided into 2, there is an image that is analog and there is an image that is digital. Analog image is an image that is continuous, such as images on television monitors, X-ray photos, and CT scan results. Meanwhile, digital images are images that can be processed by computers [8]. Image processing is a form of processing an image or image with a numerical process of the image, in this case the individual pixels or points of the image are processed. Digital image processing techniques help manipulate digital images using computers. The purpose of image processing is to improve image quality. Where the resulting image can display information clearly and extract feature information from the image. Some of the techniques used in image processing are as follows[9-11]. Brightness [12-14] is a process for adjusting the brightness of an image. If the pixel intensity is reduced by a certain value, the image will be darker and vice versa, if the pixel intensity is increased by a certain value, the image will be lighter. Brightness can be done with equation 2.1.

$$f_i(x, y) = f_j(x, y) + k \qquad \textit{(eq.2.1)}$$

Where:
fi (x, y): Pixel value at point x, y after brightness, fj (x, y): Pixel value at point x, y Original image, k: Brightness gain value. The above equation is used for grayscale images. If used in RGB images, equation 2.1 can be derived as in equations 2.2, 2.3, and 2.4.

$$fi^{R}(x, y) = fj^{R}(x, y) + k \qquad \textit{(eq.2.2)}$$
$$fi^{G}(x, y) = fj^{G}(x, y) + k \qquad \textit{(eq.2.3)}$$
$$fi^{B}(x, y) = fj^{B}(x, y) + k \qquad \textit{(eq.2.4)}$$

Where:
fi^{RGB}: Pixel value at point x, y RGB image after brightness, fj^{RGB}: Pixel value at point x, y original RGB image, k: Brightness gain value of image

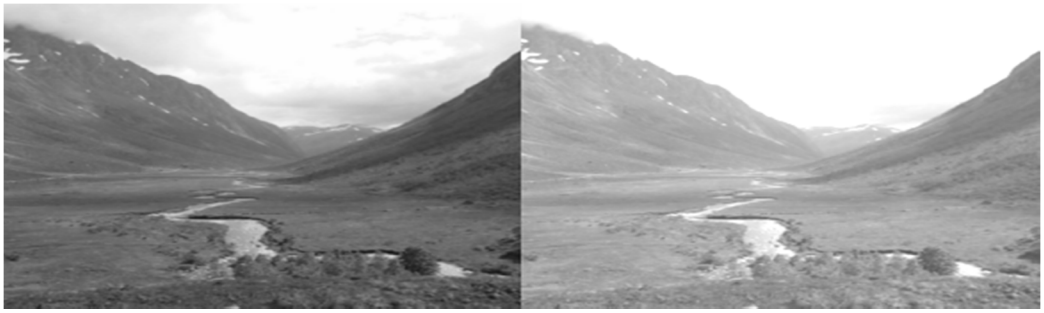

Figure 2.3: Contrast to Brightness

Median Filter [15,16] is used to remove salt & pepper type noise that is often found in retinal images. Noise has a fixed value of 0 (pepper noise) and 255 (salt noise). This noise filtering technique is divided into two, namely linear and non-linear. The most widely used non-linear filter is the Median Filter which uses the median value to replace the damaged pixels and this filter is able to remove noise without removing the edges (Shrestha, 2014). This median filter technique focuses on the median or middle value of the total number of total pixel values contained in the image. The equation used to get the median value of an image can be seen in the equation:-

$$x = \frac{n+1}{2} \qquad (eq.2.5)$$

Where:

x: New value median, n: Total data

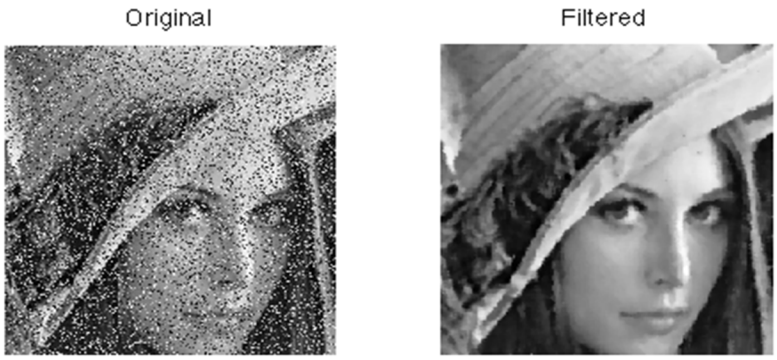

Figure 2.4: Median Filter

The grayscale technique is used to convert an RGB color image into a gray image. A gray image (grayscale) is an image where each pixel contains information on the intensity value of white and black. The lowest or no intensity value in a grayscale image is represented in black and the highest value represents white. All values between these highs and lows represent shades of gray. The number of these shadows depends on the possible values a pixel can have. if the pixel is expressed in bits, it can store two values, 0 and 1 and thus a black and white image, no grayscale. If pixels are expressed in bytes, there will be 256 gray levels starting with 0 as black and ending with 255 as white [16-23]. The results obtained from the grayscale process will make it easier for the image to be processed further in the thresholding process. The equation used to convert an RGB color image to a grayscale image can be seen in equation 2.6:

$$s = \frac{r+g+b}{3} \qquad (eq.2.6)$$

Where: s: Grayscale image, r: Red value, g: Blue value, b: Green value

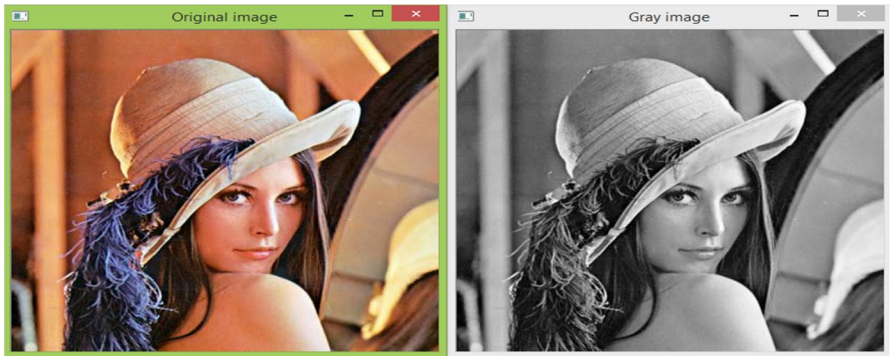

Figure 2.5: Gray Scaling

The thresholding procedure is used to adjust the degree of gray in the image which will produce a binary image [16-23]. The image has two gray levels, namely black and white. The process of determining the image color level at the thresholding is done by obtaining a threshold value. The thresholding process will change the pixel color to black if the image intensity value is less than the threshold value and if the image intensity value is more than the threshold value, the pixel color will turn white. The equation used to calculate the threshold value can be seen in equation 2.7:

$$T = \frac{fmaks + fmin}{2} \qquad (eq.2.7)$$

Where: T: Fax threshold value:, Fmaks: Maximum pixel value, Fmin: Minimum pixel value

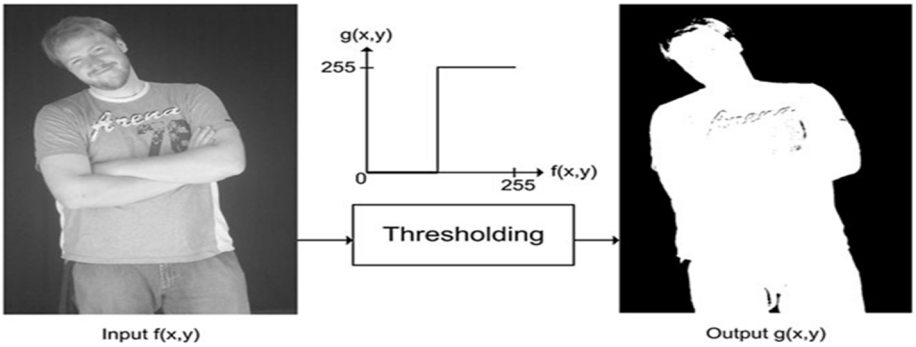

Figure 2.6: Process Thresholding

The feature withdrawal process in this case study is carried out using the Gray Level Co-occurrence Matrix (GLCM) method [16-23].GLCM is a matrix that represents the spatial distance and the relationship between two pixels in a grayscale image. GLCM is a matrix of size n × n, where n is the number of gray levels that a grayscale image has. The feature withdrawal steps using the GLCM method are as follows.

- Determine the work area of the matrix.
- Determine the distance and angle between the reference pixel and neighboring pixels. The distance (d) used is 1 and the angles (θ) used are 0^o, 45^o, 90^o, and 135^o.
- Calculates the co-occurrence value based on the distance and angle that has been determined.
- Adding the co-occurrence matrix with the transpose matrix so the co-occurrence matrix is proportioned.
- Normalize the co-occurrence matrix by dividing each co-occurrence value in the matrix by the sum of all existing co-occurrence values, so that the summation of all values in the matrix is 1.
- Calculating the statistical features of the GLCM based on Haralick features.

There are 6 characteristics used, namely contrast, homogeneity, energy, entropy, variance, and correlation.

$$\boldsymbol{p(i,j) = \frac{P_d(i,j)}{\sum_{i,j}^{N=1} P_d(i,j)} \quad (eq.2.8)}$$

Contrast is used to measure the variation of the pair of gray levels in an image.Contrast is calculated using the formula in equation 2.9:

$$\boldsymbol{Contrast = \sum_{i,j=0}^{N-1} P_{(i,j)}(i-j)^2 \quad (eq.2.9)}$$

Homogeneity is used to measure the homogeneity of images with similar gray levels. Homogeneity is calculated by the formula in equation 2.10:

$$\boldsymbol{\mathbf{Homogeneity} = \sum_{\mathrm{i,j=0}}^{\mathbf{N-1}} \frac{\mathbf{P_{(i,j)}}}{\mathbf{1 + (i-j)^2}} \quad (\mathbf{eq.2.10})}$$

Energy is used to measure the homogeneity of an image. Energy is calculated using the formula in equation 2.11:

$$\boldsymbol{Energy = \sum_{i,j=0} P\,(i-j)^2 \quad (eq.2.11)}$$

Entropy is used to calculate the level of image irregularity. Entropy is calculated using the formula in equation 2.12:

$$\boldsymbol{Entropy = \sum_{i=0}^{N-1} \sum_{j=0}^{N-1} P_{\,i,j}(i-\mu_i)^2 \quad (eq.2.12)}$$

Variance is used to measure the distribution between the mean combination between reference pixels and neighboring pixels. Variance is calculated using the formula in equation 2.13:

$$\boldsymbol{Variance \;=\; \sigma 2 = \sum_{i=0}^{N-1} \sum_{j=0}^{N-1} P_{\,i,j}(i-\mu_i)^2 \quad (eq.2.13)}$$

Correlation is used to calculate the association of pixels that have gray level i with pixels that have a gray level j. Correlation is calculated using the formula in equation 2.14:

$$Correlation = \sum_{ij} \frac{(i-\mu i)(j-\mu j)p(i,j)}{\sigma i \sigma j} \quad \textbf{(eq.2.14)}$$

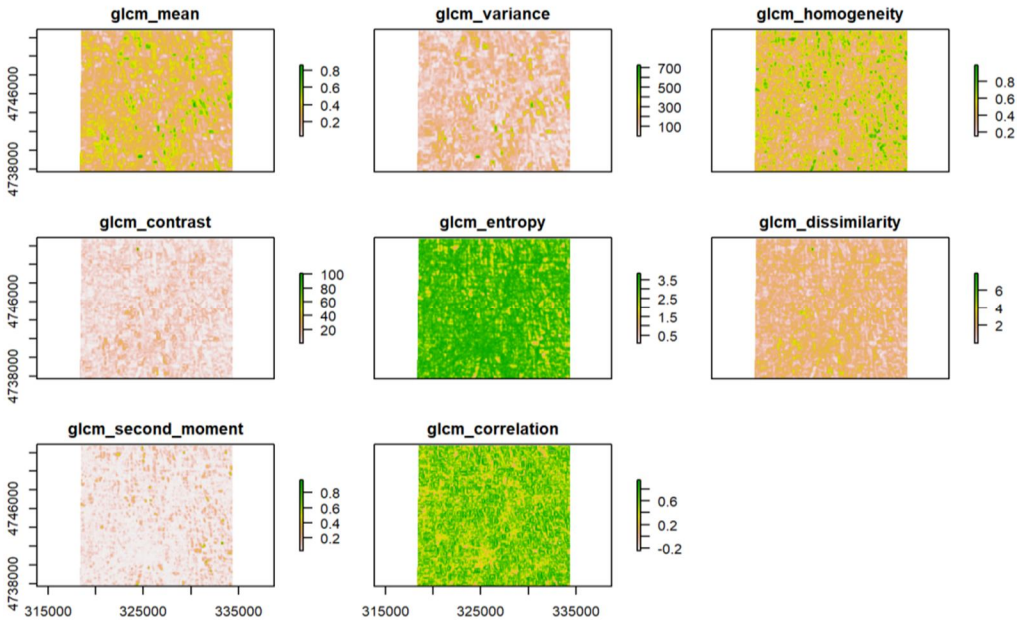

Figure 2.7: Gray Level Co-occurrence Matrix (GLCM) method

Artificial intelligence has actually started since the season heat in 1956. at that time a group of computer experts, experts and researchers from other disciplines from various academies, industry as well as various circles converged on Dartmouth College to discuss the potential of from the laboratory to real work implementation[24-27].Atfirstartificialintelligence only existed inuniversitiesand research laboratories, and very few - if any practical product that has beendeveloped. Towards the end of the year 1970s and early 1980s, began to be developed gradually full computers in order imitate or simulate human intelligence. Some the scientists involved were Allen Newel, Herbert Simon, Marvin Miskey, Oliver Selfridge, and John McCarthy. Since at that time, experts began to work hard to make,discuss, change and develop until reaching full point of progress. Starting and the results are gradually starting to be marketed. Currently, many research results are being and have been 1 converted into tangible products that bring profits for the wearer. Artificial intelligence (AI), the definition according to some experts:

1) Schalkoff (1990): AI is an endeavoring field of study describe and imitate intelligent behavior in forms computational process.
2) Rich and Knight (1991): AI is the study of means make computers do something that was, until recently this, people can do better.
3) Luger and Stubblefield (1993): AI is a branch of science computer-related behavioral automation the smart one.
4) Haag and Keen (1996): AI is a field of study that is related to capturing, modeling,and storage of human intelligence in a system information technology so that the system can facilitate the decision-making process usually done by humans.

Artificial intelligence is a technology that simulates human intelligence. Computers can quickly solve a problem by imitating how humans solve the problem. One branch of AI is focused on developing algorithms for analyzing the content of an image. Computer vision tries to imitate the workings of the human visual system. Computer vision aims to allow computers to recognize an image and make decisions. The rapid development of the internet has led to the development of an extraordinary volume of textural information. Basically, the world community is very dependent on the existence of information from various fields, be it information in the form of text, images, videos or information from a web page [28-31].

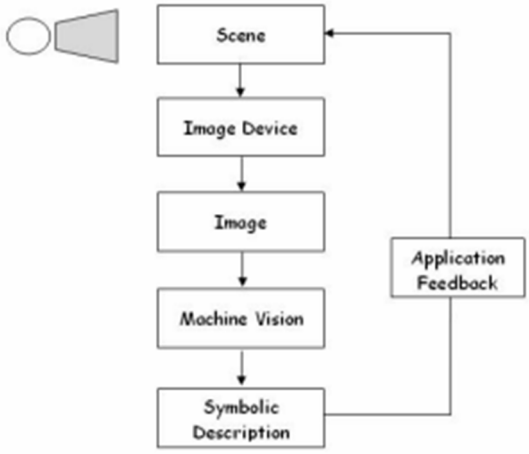

Figure 2.9: Structure of Computer Vision

Artificial Neural Network is a logical model that works based on the human brain. The workings of the brain using a number of simple neurons and interconnected with a weight value that transmits the signal from one neuron to another neuron can be modeled by an artificial neural network. Input will be received by each neuron through its connection. An output that corresponds to the weighted value of the relationship will be generated by the neuron, then the output will be forwarded back to the other neurons. Each neuron in an artificial neural network consists of several layers or layers. An artificial neural network generally consists of three layers, namely: the input layer, namely the nodes that receive the input signal, the middle layer which is also known as the hidden layer, which is the node that connects the nodes in the input layer with the nodes in the output layer and the output layer, namely nodes- the node that generates the output signal. Artificial neural networks learn by adjusting the weight values used to transmit values from one neuron to another [32-36]. Neural networks are one of the most advanced programming methods ever invented. In the conventional approach to programming, the computer is told what to do in solving a big problem by dividing it into many small precisely defined tasks so that problem solving can be done easily by the computer. On the other hand, in an artificial neural network, the computer is not told how to know which problem to solve. Instead, it learns from observational data then looks for solutions to solve problems. However, until 2006 researchers did not know how to train neural networks to be able to go beyond the computer problem solving approach in a more traditional way, except for a few specific problems [37-41]. Deep Belief Network (DBN) is one of the most popular deep learning models consisting of a number of Restricted Boltzmann Machine (RBM) layers and a Backpropagation (BP) layer. RBM is a generative model that can collect structural information in data and can effectively train non-linear data through unsupervised training. Each RBM layer extracts input data in a bottom-up manner and the output information from the last RBM layer is used as input data from the BP neural network.TheRBMtrainingprocess makesit suitable as a DBN module. The objective of DBN is to extract and separate bottom-up input data for each RBM layer and store all important information. The multi-layer RBM layer uses the unsupervised learning method,while the Backpropagation Neural Network (BNN) uses the supervised learning method. Each layer of the RBM extracts input data bottom-up and the output information from the last layer of the RBM network is used as input data at the BNN. Because the training carried out by each RBM layer can only make the parameters at that layer achieve optimization, we use BNN for top-down tuning of the entire model. Meanwhile, the information obtained from the optimization of the RBM network is used as the BNN data input which solves the problem of the BNN, namely that it is easy to fall into local minimums and has slow convergence [42-47].

$$P(H_j = 1|V) = f(B_j + \sum_{i=1}^{m} W_{ij} V_i) \qquad (2.15)$$

$$P(H_j = 1|V) = f(B_j + \sum_{i=1}^{m} W_{ij} \frac{V_i}{\sigma_i^2}) \qquad (2.16)$$

$$P(V = 1|H) = f(C_j + \sum_{i=1}^{m} W_{ij} H_i) \; (\qquad eq.2.17)$$

The Negative Phase uses Gaussian Bernoulli, so it becomes:-

$$P(V_i = V|H) = N(V|C_j + \sum_{i=1}^{m} W_{ij} H_i \sigma_i^2) \; (eq.2.18)$$

$$Updt\,(W_{ij}) = W_{ij} + L*(Positive\,(E_{ij}) - Negative\,(E_{ij})) \; (eq.2.19)$$

with derivatives

$$f_1(x) = f_1(x)\big(1 - f_1(x)\big)(eq.2.21)$$

$$\mathbf{f(x)} = \frac{\mathbf{e^{zi}}}{\sum_{\mathbf{k=1}}^{\mathbf{k}} \mathbf{e^{zj}}} \ \mathbf{(eq.2.22)}$$

$$\boldsymbol{f'(x) = (x)(1 - f(x))} \ \mathbf{(eq.2.23)}$$

The most used non-linear activation functions are the following:

$$\sigma(z) = \frac{1}{1 + e^{-z}} \ (eq.2.24)$$

- **Hyperbolic Activation Function**

$$y = \frac{e^{zx} - e^{zx}}{e^{zx} + e^{zx}} \ (eq.2.25)$$

- **Relu Function (Rectified Linear Unit)**

$$y = max(0, x)(eq.2.26)$$

The ReLU (Rectified Linear Unit - see figure 2.19 function is the most used (at the time of writing this work) and is used in almost all types of networks convolutional as well as in other types of deep learning networks. It is derivable and it is monotonic (its derivative is also monotonic). A disadvantage of the ReLU function is that the weights could be updated in a certain way in which the neuron never fires, that is, the output of that neuron is always zero and when that condition is reached during training. However, it has important advantages compared to the Sigmoid or Tangential Hyperbolic function, such as the acceleration in the convergence of the network (by means of the stochastic descending gradient) because it does not involve costly calculations in training [42-47]. Furthermore, it does not suffer from the phenomenon of gradient disappearance. This function is a variation of the ReLU function, where the values of$X$ less than 0 are mapped to a function and $y = aX$ (with to equal to a small constant and greater than 0), instead of $y = 0$ as we saw previously (see equation 2.27) [42-47].

$$\mathbf{y = max(k * x, x)\,;\, con\ 0 < k < 1}\ (eq.2.27)$$

Figure 2.20: Leaky ReLU activation function (Non-linear)

$$f \approx argmin_{f \in F}\left(\frac{1}{n} * \sum_{i=1}^{n} j(f(x_i), y_i)\right) \ (eq2.28)$$

$$J(\theta) = \left(\frac{1}{n} * \sum_{x=1}^{n} (f(x_i) - y_i)\right)^2 \ (eq2.29)$$

$$TNR = \frac{Number\ of\ true\ negatives}{Number\ of\ negative\ examples} = \frac{VN}{\mathbf{VN + FN}} (eq.3.30)$$

$$TPR = \frac{Number\ of\ true\ Positives}{Number\ of\ Positive\ examples} = \frac{VP}{\mathbf{VP + FN}} (eq.3.31)$$

$$\mathbf{F1 - Score} = 2 * \frac{Precision * Recall}{Precision + Recall} (eq.2.34)$$

$$Accuracy = \frac{Number\ of\ correct\ positive\ predictions}{Number\ of\ positive\ predictions} = \frac{VP}{\mathbf{VP + FP}} (eq.2.35)$$

The data used were 50 data. From the combination of feature extraction used by the author, the system accuracy rate for glaucoma classification results reaches 86% [51]. The study by Golob, Anna & Takahashi, Traci & Johnson, Kay [53] in the year 2020 which made the system detect the location of a tumor or breast cancer obtained an accuracy rate of 91%. The data used for this detection process uses a mammogram image with a combined data processing method of MLP algorithms and multilevel threshold. Medical images were obtained from the segmentation results, namely the gray image which was used as input in the extraction process using CNN and RGB images used in the process of determining the location of a tumor or cancer.

Another D. Varshni, K. Thakral, L. Agarwal, R. Nijhawan and A. Mittal [54] in the year 2019 methodology used by the authors works under an architecture of densely connected neural network or known as DenseNet-169. The authors determined that the ideal feature extraction architecture to support loss of gradient is DenseNet-169, as your pre-trained network consists of 169 layers of equal sizes directly to each other. In the last phase, the classification, different techniques were used such as Support Vector Machine (SVM), Random Forest, Naive Bayes, K- nearest, among others. Research determined that the combination of the DenseNet-169 architecture as a feature extractor and SVM as the classifier. Research by Torres, C. and López, C., [55] in the year 2019 proposed a model for the classification of cases of schizophrenia through electroencephalography (EEG) signal analysis with the use of deep learning methods. Using other studies carried out for the same type of disease using trait classifiers such as Random Forest, they realized that the information obtained from the characteristics of EGG signals are of high dimensionality, variability and multichannel, for which they proposed to apply the technique of Pearson's correlation coefficient (PCC), thereby reducing this type of characteristics and bring them to a heat matrix that could serve as input for a neural network convolutional. Finally, the results that his study shows are based on metrics of precision, specificity and sensitivity. The ultimate goal is to establish a prediction model with techniques such as PCC for precision in the diagnosis and classification of different mental illnesses that use EGG signals.

II. PROPOSED METHODOLOGY

This chapter will discuss the analysis and design of glaucoma identification applications. The analysis stage discusses the steps taken to identify glaucoma starting from the data analysis stage, the prepocessing stage to the identification stage using the Deep Belief Network. At the next design stage, the system interface display design will be carried out.

A. General Architecture

This section will discuss the steps involved in developing a glaucoma identification application. The steps taken are as follows: the stage of collecting fundus image data consisting of normal images and glaucoma images which will be used as training data and test data; the prepocessing stage consisting of brightness, median filter, grayscale, and thresholding; the image feature extraction stage uses the Gray Level Co-occurrence Matrix (GLCM); and the image classification stage using the Deep Belief Network. After these steps are carried out, the application can produce output in the form of glaucoma identification results. The stages can be seen in the form of a general architecture in Figure 2.1. Figure 3.1 is an overview of the general architecture of the research classification using deep learning with an adaptive learning rate. The initial process is to collect data related to the data to be examined, then normalized and transformed the dataso as to produce data that is ready to be tested. Furthermore, the data is divided into two namely data for training and data for testing. Classification process using a standard deep neural network on the one hand, and on the other using a deep neural network with an adaptive learning rate. The training process the deep neural network has 2 training phases, the first phase is unsupervised learning deep belief network, and the second phase of supervised learning fine-tuning deep neural network. The final result of the classification will be analyzed for each of its performance.

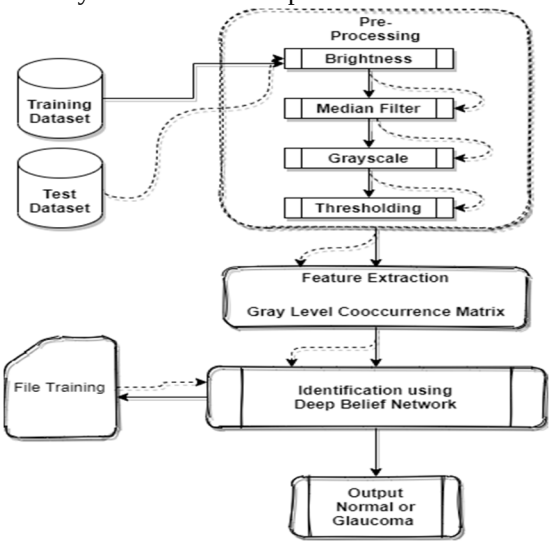

Figure 2.1: Proposed Architecture

B. Preprocessing Data

The data preprocessing stage is the stage of data selection that aims to get data that is suitable for use. The value is often found in raw data missing value, not stored value (misrecording), data sampling which is not good enough and whatnot. Therefore it takes steps like discard some records that will not be analyzed or that do not becomedeterminants of data classification and transformation.

- *Data Transformation*

Data transformation was carried out to obtain the overall value for each attributewith a scale of 0 to 1 so that the analysis process is easier to do. The value transformation in the data uses the following equation:

$$\textbf{NewValue} = \frac{\textbf{Old Value} - \textbf{Min Value}}{\textbf{Max Value} - \textbf{Min Value}} (\textbf{Range Max} - \textbf{Range Min}) + \textit{Range Min} \qquad (1)$$

- *Data Set*

The data used in this study are fundus images consisting of normal images and glaucoma images. This data was obtained from the RIM-ONE database (http://medimrg.webs.ull.es). RIM-ONE is a retinal fundus image database developed by 3 hospitals, namely Hospital Universitario de Canarias, Hospital Clinico San Carlos, and Hospital Universitario Miguel Servet. The types of images used in this study are normal fundus images and glaucoma fundus images. In Figure 3.2 part (a) is a normal fundus image and in part (b) is a glaucoma fundus image.

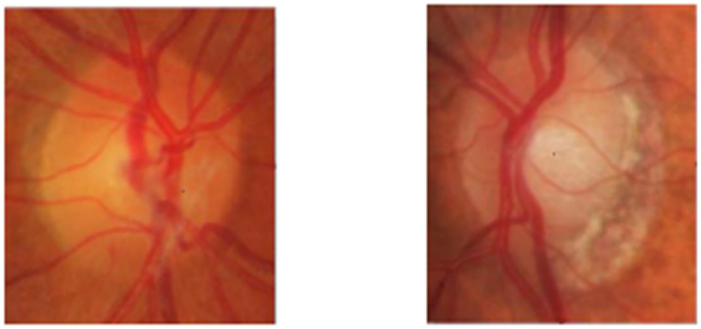

Figure 2.2 (a) Normal Fundus Image (b) Fundus Glaucoma Image

In the pre-processing stage, several processes are carried out to produce an image that is it is better to process it at a later stage. The pre-pocessing stage is brightness, median filter, grayscale, and thresholding.

1) Brightness

Image brightness is the step to adjust the brightness of an image. This stage done to increase the brightness of the image so that the optical disc looks even more it is clear where this stage is carried out so that the image can be more easily processed at the stage next. It can be seen in Figure 3.3 part (a) is an original image that has not been processed and part (b) is the result of the brightness enhancement process carried out on original image.

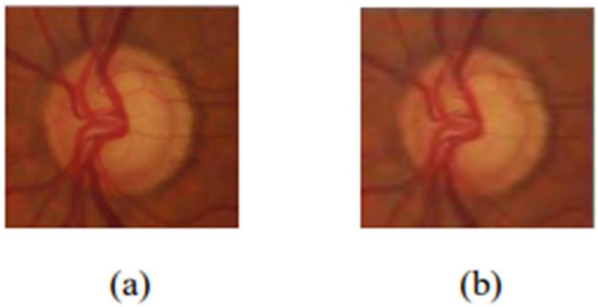

Figure 2.3 (a) Original Image (b) Image Result of Brightness

2) Median Filter

This stage is done to remove salt & pepper type noise that is often found in the image. Median filter works by processing every pixel in the image then replacing each pixel value with the nearest pixel median value. The pattern of the median value of the surrounding pixels is called a window. Figure 3.4 is the image resulting from the median filter.

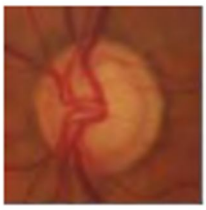

Figure 2.4 Image of Median Filter Result

3) Grayscale

Fundus image which is an RGB color image will then be converted into a gray image by utilizing the grayscaling process. In Figure 3.5, you can see the image of the grayscale process.

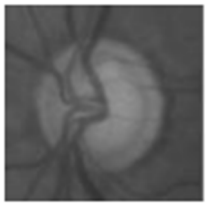

Figure 2.5 Grayscale Result Image

4) Thresholding

5)

The thresholding stage is carried out to change the gray image into a binary image is worth 0 (black) and 1 (white). The image areas that tend to be dark will be changed becomes black (intensity value 0) and an area of the image that tends to be bright is created becomes white (intensity value 1). Figure 3.6 shows the image of the thresholding result.

Figure 2.6 Thresholding Result Image

C. Feature Extraction

After going through the preprocessing stage, the next step is the extraction stage feature (feature extraction). The feature extraction method used in this study is the Gray Level Co-occurrence Matrix (GLCM). Here are the steps feature extraction using GLCM.

1) Forming a framework matrix using the degree of gray value (gray level) image. The gray level value used is 256.
2) Determine the track and distance between one pixel and the surrounding pixels. Distance cast-off is 1 and the direction used is 0^o , 45^o , 90^o , and 135^o.
3) Calculating the co-occurrence value based on the predetermined direction and distance.
4) Adding the co-occurrence matrix with the transpose matrix so that the matrix co-insurance to be symmetrical.
5) Normalize the co-occurrence matrix that is in symmetrical form with how to divide the co-occurrence value in the matrix by the total number of values the existing co-occurrence standards, so that the summation of all the values is 1.
6) Compute the value of the features of the GLCM. There are 6 features used, namely contrast, consistency, energy, entropy, variance, and relationship.

The co-occurrence matrix is calculated based on 1 distance and 4 directions, then the value of 6 features calculated for each co-occurrence matrix that has been normalized, so that there will be 24 features produced. An example of a feature value from a retinal image in Figure 2.6. shown in Table 1

NO.	VALUE	DIRECTION	FEATURE
1	CONTRAST	0^{O}	3.17613
2	CONTRAST	45^{O}	6.65454
3	CONTRAST	90^{O}	4.04741
4	CONTRAST	135^{O}	6.40902
5	HOMOGENEITY	0^{O}	0.56575
6	HOMOGENEITY	45^{O}	0.45288
7	HOMOGENEITY	90^{O}	0.53827
8	HOMOGENEITY	135^{O}	0.45637
9	ENERGY	0^{O}	0.00642
10	ENERGY	45^{O}	0.00452
11	ENERGY	90^{O}	0.00584
12	ENERGY	135^{O}	0.00456
13	ENTROPY	0^{O}	5.62852
14	ENTROPY	45^{O}	5.9894
15	ENTROPY	90^{O}	574,635
16	ENTROPY	135^{O}	5.97009
17	VARIANCE	0^{O}	145.3995
18	VARIANCE	45^{O}	144.0876
19	VARIANCE	90^{O}	145.5577
20	VARIANCE	135^{O}	144.749
21	CORRELATION	0^{O}	0.98908
22	CORRELATION	45^{O}	0.97691
23	CORRELATION	90^{O}	0.9861
24	CORRELATION	135^{O}	0.97786

Table 1 GLCM Features

D. *Proposed Algorithm*

The next step after getting the GLCM feature value is image identification via Deep Belief Network (DBN) method. The preliminary stage carried out in the image identification procedure is the training dataset training process. In this case study, researcherscast-off 80 input data to be trained. The Restricted Boltzmann Machine (RBM) algorithm is also used during the training process.

The parameters used in the DBN method are:

- Determine the number of visible nodes. In this study, there are 3 nodes takenfrom the characteristics of glaucoma images, namely optical disc, optic cup, and vesselsretinal blood.
- Determine the number of hidden nodes. In this study there are 2 nodes determined because the results were normal and glaucoma.
- Determine the value of the learning rate. The value specified is 0.1.
- Determine the momentum value. The value specified is 0.5.
- Determine the unsupervised epoch value.
- Determine the supervised epoch value.

1) Determining the Network Architecture

Before data processing, it is necessary to determine the network architecture, such as determining the number of layers used, the number of neurons in each layer used, the activation function used, and other parameter values.

a. Input layer Based on the attributes to be used, there are contrast, homogeneity, energy, variance and correlations like attributes that will be used as neuron input.
b. Hidden layer / dense layer In a neural network, it is generally not more than 2 layers, but in deep learning it is possible to have more than two hidden layers. However two layers can also be used for simple datasets. There are three rules in choosing the number of neurons in each hidden layer
   1. The number of neurons between the input and output sizes of neurons
   2. The number of neurons is 2/3 of the input neurons plus the output of the neurons
   3. The number of neurons is less than 2 times the input of neurons From the above criteria, this study will use 2 hidden layers with 9 neurons on each layer.
c. Output layer Generally, the number of neurons in the output layer depends on the classification problem. This study includes a multi-class classification, which will classify three types of mangrove sprouts, so that the number of neurons in the output layer is 3.
d. Activation function The activation function commonly used in classification on neural networks with a value between 0-1 is the sigmoid activation function, but the sigmoid activation function is generally used for binary classification. This study uses a multi-class classification which has 3 neurons in the output layer. The softmax activation function can be used in multi-class classification which has an output of more than 2 neurons, this activation function is generally used at the output layer in a neural network. So this research uses the sigmoid activation function in the hidden layer, and the softmax activation function in the output layer.
e. Parameters Parameters such as weights and bias used are random, and the learning rate used is 0.1. Other parameters in this study such as momentum are not used, this is based on the use of standard values of momentum on several problems that cannot have a major effect, such as doing a combination with softmax. Architectural specifications to be built is depicted below.

2) Steps for Training using DBN

The deep belief network (DBN) that has been trained in the first phase of training will be transformed into a deep neural network (DNN) by adding a discriminative layer *y* at the top layer of the RBM, then changing the connection within the DBN (from two directions to one direction) becomes feed-forward. The parameters that have been previously estimated by DBN can be used directly as DNN parameters, or can also be improved, for example by applying the backpropagation algorithm. The flow of the backpropagation algorithm is as follows:

1. Using the same number of neurons and structures as the DBN that was pre-trained using the Contrastive Divergence algorithm in the first training phase.
2. Change the direction of the weight which was originally two-way or not directional to one direction like the Multi-layer Perceptron
3. Set weight for each weight and bias is the final weight in the DBN Contrastive Divergence process above.

Feed Forward

4. Each hidden unit (Z_j) receives a signal from each input unit (X_i) with the following equation.

$$Z\_netj = vjo + \sum_{i=1}^{n} xivj$$

Use the activation function to calculate the output signal:

$$Z_j = f\,(Z\_net_j)$$

And send the signal to all the upper layer units(output units).

Thisstepisdone as many as the number of hidden layers.

1. Calculate all network outputs in the output layer($Y_k, k = 1,2, \ldots, m$)
2.

$$Y\_net_k = w_{k0} + \sum_{j=1}^{p} z_j w_{kj}$$

This section contains implementation and testing of applications based on analysis and system design that has been discussed in the previous chapter. This stage aims to displays the results of the system design that has been built and the testing process a system for identifying glaucoma.

E. Application Requirements

In designing the glaucoma disease identification application through fundus images using the Deep Belief Network requires both hardware and software supporters include:

1) Hardware

The hardware specifications used in this application are:

- *a)* 6 Core vCPU VM Processor (2 units)
- *b)* 2 Core vCPU VM Processor
- *c)* 56 GB DDR4 RAM (2 units)
- *d)* 8GB DDR4 RAM
- *e)* 340 GB Temporary Storage (2 units)
- *f)* 110 GB SSD Storage (3 units)
- *g)* Nvidia Tesla K80 (2 units)

2) Software

The software specifications required in this study include:

- *a)* CentOS6.064 bit Operating System [Server].
- *b)* Windows 10 64 bit Operating System along with Browser (Chrome) [Client].
- *c)* Anaconda Python 3.6.
- *d)* Library: Pandas,Numpy, Matplotlib, PIL, Keras, Tensorflow, OpenCV.
- *e)* Jupyter Notebook

3) Data Implementation

This study uses a dataset in the form of digital images derived from retinal photographs. The dataset obtained is sourced from an online data science and artificial intelligence platform called RIM-ONE dataset (http://medimrg.webs.ull.es) however the same data is also available on kaggle.com. From these data, the classification can be divided into 2 categories of eye blindness, namely normal and glaucoma.

4) Preprocessing

To start the research, pre-processing was carried out which consisted of several stages. Pre-processing is done to convert digital raw into digital images that are ideal for the training process. The first thing to do is to make sure the dataset used has a label for the type of blindness that each eye has and can be used for the training process. The data that has been prepared must be visualized to show the eye and the type of label as shown below.

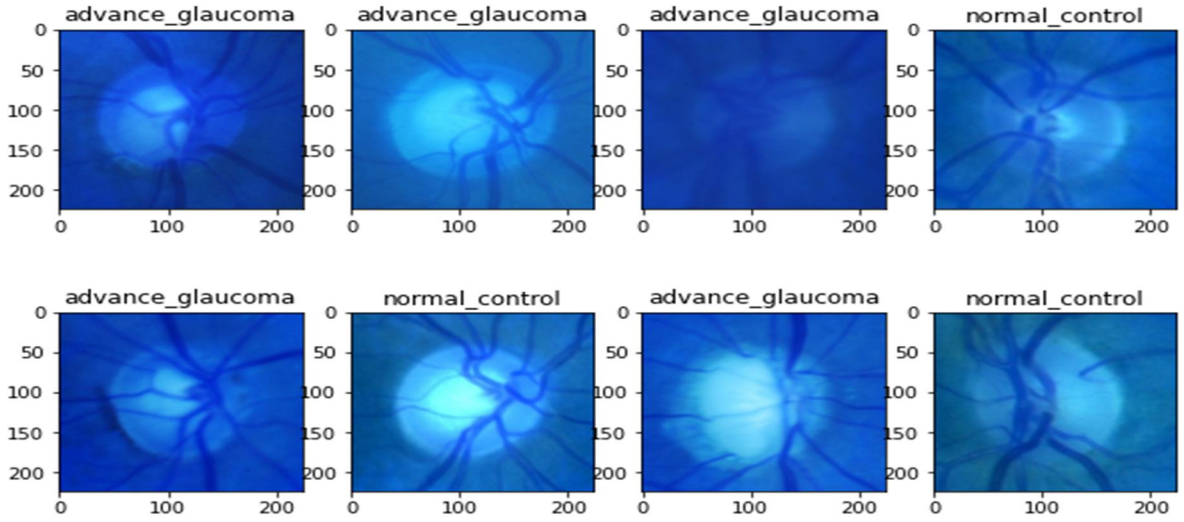

Figure 2.7: Fundus Images (Dataset)

From the results of the visualization above, it can be ascertained that the data used already has a label and is a dataset that is in accordance with the needs of this study. Then the thing that must be done is pre-processing so that the dataset becomes an ideal dataset so that there are no obstacles in the training process.

5) Brightness

This stage increases the brightness of the image so that the optical disc looks even more it is clear where this stage is carried out so that the image can be more easily processed at the stage next.

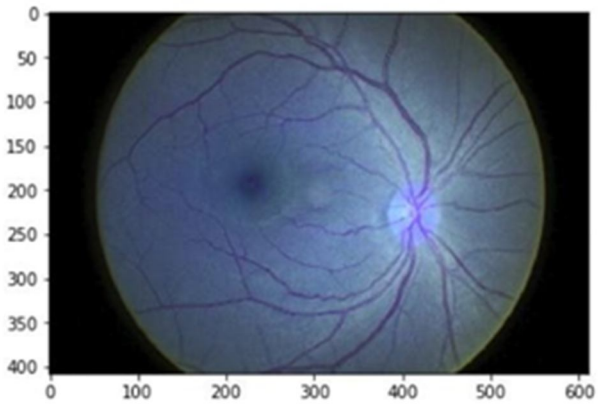

Figure 2.8 Brightened Retina Image

6) Median Filter

Median filter functions to remove noise in the image. Noise removal is carried out in order to produce better quality images. The filter used with 2D images as under:

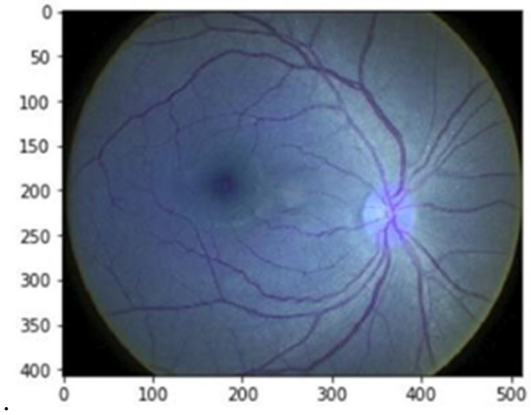

Figure 2.9: Filtered Retina Image

7) Grayscale

Grayscale means a process to turn an eye digital image into a monochromatic digital image. In this study, the purpose of carrying out the grayscale process is to ensure that the eye anomaly that has been described as a parameter can be seen when the training process is in progress. At this stage the grayscale process is carried out using the gaussian blur method. The gaussian method is combined with the image blending process. The image blending formula used is as follows.

$$g(x) = (1 - \alpha) .f_0(x) + \alpha f_1(x)$$

The image blending process with the Gaussian blur method allows for several variations. Variation is carried out at α using a value between 0 and 1. The process of changes can produce different transformations depending on the type of requirement.

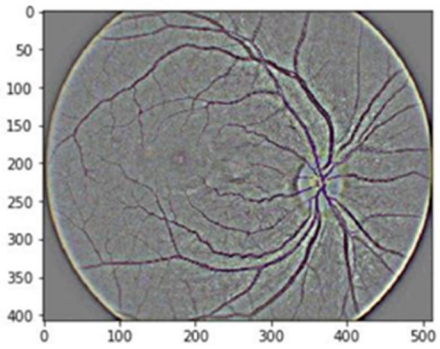

Figure 2.10 Retina Image Converted to Grayscale

F. GLCM

The extraction of second-order statistical features is carried out with a co-occurrence matrix, which is an intermediate matrix that represents the adjacency relationship between pixels in an image in various orientations and spatial distances . The co-occurrence matrix is a matrix of size *L x L* (*L* represents the number of gray levels) with the element $P(x_1, x_2)$ which is a joint probability distribution of a pair of points with a gray level x_1 located at coordinates (j, k) where x_2 is located at coordinates (m, n). The coordinates of the pair of points are r with the angle θ. Thesecondlevelhistogram $P(x_1, x_2)$ is calculated with the following approximation results.

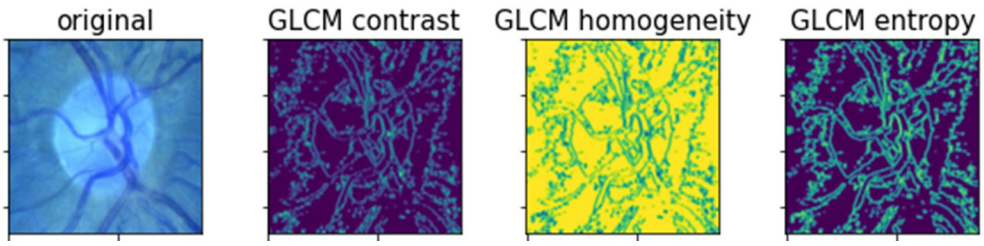

Figure 2.11 Feature Extraction using GLCM

G. System Testing using DBN

System testing is carried out to determine the ability of the system that is built to identify fundus images. The system's ability to identify fundus images depends on the training process using the Deep Belief Network because the training procedure produces the final weights that will be used in the testing phase. Previously, 66 glaucoma images and 66 normal images were tested with different epoch parameters. The graph of the system accuracy value after testing 40 images with different epoch parameters havebe see in Figure 4.6. From tests carried out by different epoch parameter standards as under with accuracy of 98.00%.

```
Trainable params: 12,673,261
Non-trainable params: 2,542
_________________________________________________________________
Epoch 1/100
9/9 [==============================] - 113s 12s/step - loss: 0.7269 - accuracy: 0.6481 - val_loss: 5.0366 - val_accuracy
Epoch 2/100
9/9 [==============================] - 101s 11s/step - loss: 0.3157 - accuracy: 0.8878 - val_loss: 5.3591 - val_accuracy
Epoch 3/100
9/9 [==============================] - 102s 11s/step - loss: 0.2742 - accuracy: 0.8896 - val_loss: 3.7417 - val_accuracy
Epoch 4/100
9/9 [==============================] - 102s 11s/step - loss: 0.2503 - accuracy: 0.9248 - val_loss: 1.6892 - val_accuracy
Epoch 5/100
9/9 [==============================] - 102s 11s/step - loss: 0.2120 - accuracy: 0.9427 - val_loss: 2.2289 - val_accuracy
Epoch 6/100
9/9 [==============================] - 102s 11s/step - loss: 0.1835 - accuracy: 0.9605 - val_loss: 1.5533 - val_accuracy
Epoch 7/100
9/9 [==============================] - 109s 12s/step - loss: 0.2091 - accuracy: 0.9385 - val_loss: 1.1183 - val_accuracy
Epoch 8/100
9/9 [==============================] - 102s 11s/step - loss: 0.1840 - accuracy: 0.9476 - val_loss: 0.7776 - val_accuracy
```

```
Epoch 20/100
9/9 [==============================] - 102s 11s/step - loss: 0.1256 - accuracy: 0.9740 - val_loss: 0.2233 - val_accuracy
Epoch 21/100
9/9 [==============================] - 111s 12s/step - loss: 0.0888 - accuracy: 0.9810 - val_loss: 0.2376 - val_accuracy
Epoch 22/100
9/9 [==============================] - 100s 11s/step - loss: 0.0990 - accuracy: 0.9745 - val_loss: 0.5807 - val_accuracy
Epoch 23/100
9/9 [==============================] - 101s 11s/step - loss: 0.0903 - accuracy: 0.9831 - val_loss: 0.6280 - val_accuracy
Epoch 24/100
9/9 [==============================] - 102s 11s/step - loss: 0.1011 - accuracy: 0.9799 - val_loss: 0.1000 - val_accuracy
Epoch 25/100
9/9 [==============================] - 101s 11s/step - loss: 0.0897 - accuracy: 0.9813 - val_loss: 0.1277 - val_accuracy
Epoch 26/100
9/9 [==============================] - 100s 11s/step - loss: 0.0934 - accuracy: 0.9744 - val_loss: 0.3961 - val_accuracy
Epoch 27/100
9/9 [==============================] - 101s 11s/step - loss: 0.0665 - accuracy: 0.9939 - val_loss: 0.1938 - val_accuracy
Epoch 28/100
1/9 [==>...........................] - ETA: 1:40 - loss: 0.1001 - accuracy: 0.9844
```

Figure 2.12 Network Training using Epoch's

1) Confusion Matrix

Based on the system evaluation score using confusion matrix, the system is considered quite effective in identifying glaucoma through fundus images using the method that has been applied to the system. The system achieves a precision in advance glaucoma the precision score of 99%, recall of 100%, and the f1 score of 99% whereas in normal control or glaucoma the precision score of 100%, recall of 98%, and the f1 score of 99% and the overall system accuracy score of 99.0%.

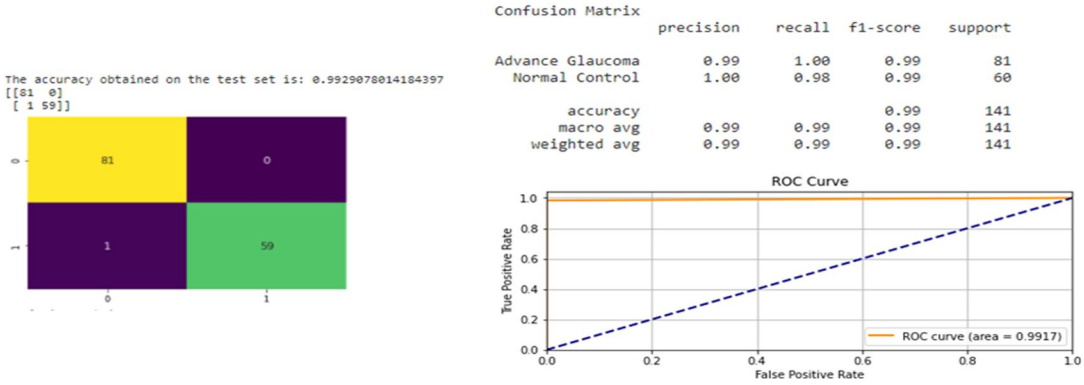

Figure 2.13: Result Illustration using Confusion Matrix and ROC

Based on the results of the experiment from this study, it can be concluded that the use of the Deep Belief Network architectural model results in a maximum and linear change in process. The results of research using Deep Belief Network produce a more rational accuracy when compared to other Neural Architectural models as student in literature with several iterations of almost 99% of accuracy. Therefore, this scheme can act as defacto standard for Glaucoma Detection.

III. CONCLUSIONS AND SUGGESTIONS

The conclusions and suggestions obtained in building an application for glaucoma identification through fundus images using the Deep Belief Network.

A. Conclusion

The conclusions that can be drawn from the results of testing the identification of glaucoma through fundus images using the Deep Belief Network are as follows:

1) The Deep Belief Network method is able to identify glaucoma through fundus images well. The results of the identification process of glaucoma through fundus images with an advance glaucoma the precision score of 99%, recall of 100%, and the f1 score of 99% whereas in normal control or glaucoma the precision score of 100%, recall of 98%, and the f1 score of 99% and the overall system accuracy score of 99.0%.

2) The selection of DBN parameter values has an influence on the accuracy results. The parameters used are supervised epoch 100.

3) The difference in the values used for the parameters also affects the duration of the training. The higher the epoch value, the longer the training data will be.

B. Suggestions

The suggestions that can be given by the author regarding this research for further development are as follows:

1) Using other neural network methods to compare with the classification results obtained from the Deep Belief Network method.

2) Inculcate the layers which can reduce the training time with same level of accuracy.

REFERENCES

[1] https://www.medicinenet.com/glaucoma/article.htm
[2] https://www.mayoclinic.org/diseases-conditions/glaucoma/symptoms-causes/syc-20372839
[3] https://www.webmd.com/eye-health/glaucoma-eyes
[4] Karegowda, Asha &Nasiha, Asfiya& M.A, Jayaram & Manjunath, A.. (2011). Exudates Detection in Retinal Images using Back Propagation Neural Network. International Journal of Computer Applications. 25. 10.5120/3011-4062.
[5] Li, Yunghui& Yeh, Nai-Ning & Chen, Shih-Jen & Chung, Yu-Chien. (2019). Computer-Assisted Diagnosis for Diabetic Retinopathy Based on Fundus Images Using Deep Convolutional Neural Network. Mobile Information Systems. 2019. 1-14. 10.1155/2019/6142839.
[6] T. Khalil, M. U. Akram, H. Raja, A. Jameel and I. Basit, "Detection of Glaucoma Using Cup to Disc Ratio From Spectral Domain Optical Coherence Tomography Images," in IEEE Access, vol. 6, pp. 4560-4576, 2018, doi: 10.1109/ACCESS.2018.2791427.
[7] Ahmad, Jamil & Muhammad, Jan & Aziz, Lubna&Ayub, Sara &Akram, M. & Basit, Imran. (2016). Glaucoma detection through optic disc and cup segmentation using K-mean clustering. 143-147. 10.1109/ICECUBE.2016.7495212.
[8] Galperin, Yevgeniy. (2021). Introduction to Basics of Digital Images. 10.1201/9780429400612-1.
[9] Gan, Woon. (2020). Digital Image Processing. 10.1007/978-981-10-5550-8_10.
[10] Seeram, Euclid. (2021). Digital Image Processing Concepts. 10.1007/978-981-15-6522-9_2.
[11] Reis, George. (2017). Digital Image Processing. 10.4324/9781315693125-12.
[12] Rizani, Fitri. (2021). IMAGE QUALITY IMPROVEMENT USING IMAGE PROCESSING METHOD IMAGE BRIGHTNESS CONTRAST AND IMAGE SHARPENING. MULTICA SCIENCE AND TECHNOLOGY (MST). 1. 6-12. 10.47002/mst.v1i1.200.
[13] Kuznetsov, Yuri. (2021). Image Processing. 10.1007/978-3-030-60955-9_2.
[14] Zielinski, Tomasz. (2021). Image Processing. 10.1007/978-3-030-49256-4_16.
[15] Micek, J. &Kapitulík, Ján. (2003). Median filter. Journal of Information, Control and Management Systems. 1.
[16] Pitas, I. &Venetsanopoulos, A.. (1990). Median Filters. 10.1007/978-1-4757-6017-0_4.
[17] Kumar, Abhishek &bhargava, Prof.Neeeaj. (2016). A Practical approach for image processing & computer vision in MATLAB.
[18] Bhargav, Dr.Neeraj& BHARGAV, Dr.Ritu& Kumar, Abhishek. (2016). A Practical Approach of Image Processing &Computer Vision in MATLAB.
[19] Rahman, Mansib. (2017). Computer Vision & Image Processing. 10.1007/978-1-4842-2316-1_6.
[20] Shapiro, Linda & Rosenfeld, Azriel. (1992). Computer vision and image processing..
[21] Marques, Oge. (2020). Image Processing and Computer Vision in iOS. 10.1007/978-3-030-54032-6.
[22] Fisher, Robert & Dawson-Howe, K & Fitzgibbon, Andrew & Robertson, C & Trucco, Emanuele. (2005). Dictionary of Computer Vision and Image Processing. 10.1002/0470016302.
[23] Parker, James. (1997). Algorithms for Image Processing and Computer Vision.
[24] Eisner, Howard. (2021). Artificial Intelligence. 10.1201/9781003160618-8.
[25] Lang, Volker. (2021). Artificial Intelligence. 10.1007/978-1-4842-6774-5_4.
[26] C.R, Rathish. (2021). Artificial Intelligence.
[27] Monte-Serrat or Monte Serrat, Dionéia&Cattani, Carlo. (2021). Artificial intelligence. 10.1016/B978-0-12-824118-9.00009-6.
[28] Szeliski, Richard. (2010). Computer Vision: Algorithms and Applications (Texts in Computer Science).
[29] Szeliski, Richard. (2011). Computer Vision: Algorithms and Applications. 10.1007/978-1-84882-935-0.
[30] Zhang, Xin & Xu, Shuo. (2020). Research on Image Processing Technology of Computer Vision Algorithm. 122-124. 10.1109/CVIDL51233.2020.00030.
[31] Prince, Dr. (2012). Computer Vision: Models, Learning, and Inference.
[32] Perros, Harry. (2021). Artificial Neural Networks. 10.1201/9781003139041-10.
[33] Cartwright, Hugh. (2021). Artificial Neural Networks. 10.1007/978-1-0716-0826-5.
[34] Okwu, Modestus &Tartibu, Lagouge. (2020). Artificial Neural Network. 10.1007/978-3-030-61111-8_14.
[35] Czischek, Stefanie. (2020). Artificial Neural Networks. 10.1007/978-3-030-52715-0_3.
[36] Bell, Jason. (2020). Artificial Neural Networks. 10.1002/9781119642183.ch9.
[37] Baldi, Pierre. (2021). Deep Learning in Science. 10.1017/9781108955652.
[38] Watson, Samuel. (2020). Deep Learning. 10.1201/9780429398292-9.
[39] Karimi, Zohreh. (2021). What is Deep Learning?.
[40] Paper, David. (2021). Introduction to Deep Learning. 10.1007/978-1-4842-6649-6_1.
[41] Ketkar, Nikhil &Moolayil, Jojo. (2021). Deep Learning with Python: Learn Best Practices of Deep Learning Models with PyTorch. 10.1007/978-1-4842-5364-9.
[42] Khan, Asifullah& Islam, muhammad. (2016). Deep Belief Networks. 10.13140/RG.2.2.17217.15200.
[43] Lopes, Noel & Ribeiro, Bernardete. (2015). Deep Belief Networks (DBNs). 10.1007/978-3-319-06938-8_8.
[44] Hua, Yuming& Guo, Junhai& Zhao, Hua. (2015). Deep Belief Networks and deep learning. Proceedings of 2015 International Conference on Intelligent Computing and Internet of Things, ICIT 2015. 1-4. 10.1109/ICAIOT.2015.7111524.
[45] Koo, Jaehoon&Klabjan, Diego. (2020). Improved Classification Based on Deep Belief Networks. 10.1007/978-3-030-61609-0_43.
[46] Mclaughlin, Tom & Le, Mai &Bayanbat, Naran. (2021). Emotion Recognition with Deep-Belief Networks.
[47] Fan, Rong & Hu, Wenxin. (2017). Face recognition with improved deep belief networks. 1822-1826. 10.1109/FSKD.2017.8393043.

[48] Nayak, Jagadish & Acharya, U Rajendra & Bhat, P & Shetty, Nakul & Lim, Teik-Cheng. (2009). Automated Diagnosis of Glaucoma Using Digital Fundus Images. Journal of medical systems. 33. 337-46. 10.1007/s10916-008-9195-z.
[49] Sengar, N., Dutta, M.K., Burget, R. &Ranjoha, M. 2017. Automatic Detection of Suspected Glaucoma in Digital Fundus Images. 2017 40th International Conference on Telecommunications and Signal Processing (TSP).
[50] Atheesan, S. &Yashothara, S. 2016. Automatic Glaucoma Detection by Using Funduscopic Images. IEEE Wispnet 2016 Conference.
[51] S Kumar and D. Singh, Energy and exergy analysis of active solar stills using compound parabolic concentrator, International Research Journal of Engineering and Technology (IRJET), 6 (2019) 12.
[52] R. Shanker, D. Singh, D. B. Singh "Performance analysis of C.I. engine using biodiesel fuel by modifying injection timing and injection pressure" International Research Journal of Engineering and Technology(IRJET) 6 (2019) 12.
[53] A. K. Anup and D. Singh, FEA analysis of refrigerator compartment for optimizing thermal efficiency, International Journal of Mechanical and Production Engineering Research and Development, 10 (2020) 3, 3951-3972.
[54] S Kumar and D. Singh, Optimizing thermal behavior of compact heat exchanger, International Journal of Mechanical and Production Engineering Research and Development, 10 (2020) 3, 8113-8130.
[55] Dharamveer and Samsher, Comparative analyses energy matrices and enviro-economics for active and passive solar still, materialstoday: proceedings, https://doi.org/10.1016/j.matpr.2020.10.001 (2020).
[56] Dharamveer, Samsher, Anil Kumar, Analytical study of N^{th} identical photovoltaic thermal (PVT) compound parabolic concentrator (CPC) active double slope solar distiller with helical coiled heat exchanger using C_uO Nanoparticles, Desalination and water treatment, 233 (2021) 30-51, https://doi.org/10.5004/dwt.2021.27526
[57] Dharamveer, Samsher, Anil Kumar, Performance analysis of N-identical PVT-CPC collectors an active single slope solar distiller with a helically coiled heat exchanger using CuO nanoparticles, Water supply, October 2021, SCI-E Index, IWA Publication. I.F 1.275,https://doi.org/10.2166/ws.2021.348
[58] M. Kumar and Dharamveer Singh, Comparative analysis of single phase microchannel for heat flow Experimental and using CFD, International Journal of Research in Engineering and Science (IJRES), 10 (2022) 03, 44-58.
[59] Kavya, N. &Katmaja, Dr. K.V. 2017. Glaucoma Detection Using Texture Features Extraction. 2017 51st Asilomar Conference on Signals, Systems, and Computers.
[60] Hyde, Kayleigh & Novack, Marlena & LaHaye, Nick &Parlett-Pelleriti, Chelsea &Anden, Raymond & Dixon, Dennis &Linstead, Erik. (2019). Applications of Supervised Machine Learning in Autism Spectrum Disorder Research: A Review. Review Journal of Autism and Developmental Disorders. 6. 10.1007/s40489-019-00158-x.
[61] Golob, Anna & Takahashi, Traci & Johnson, Kay.(2020).Breast Cancer Screening.10.1007/978-3-030-50695-7_18.
[62] Varshni, K. Thakral, L. Agarwal, R. Nijhawan and A. Mittal, "Pneumonia Detection Using CNN based Feature Extraction,"2019IEEEInternational Conferenceon Electrical,Computer and Communication Technologies (ICECCT),2019,pp.1-7,doi:10.1109/ICECCT.2019.8869364.
[63] Carlos Alberto Torres Naira and Cristian Jos´eL´opez Del Alamo, "Classification of People who Suffer Schizophrenia and Healthy People by EEG Signals using Deep Learning" International Journal of Advanced Computer Science and Applications(IJACSA), 10(10), 2019. http://dx.doi.org/10.14569/IJACSA.2019.0101067

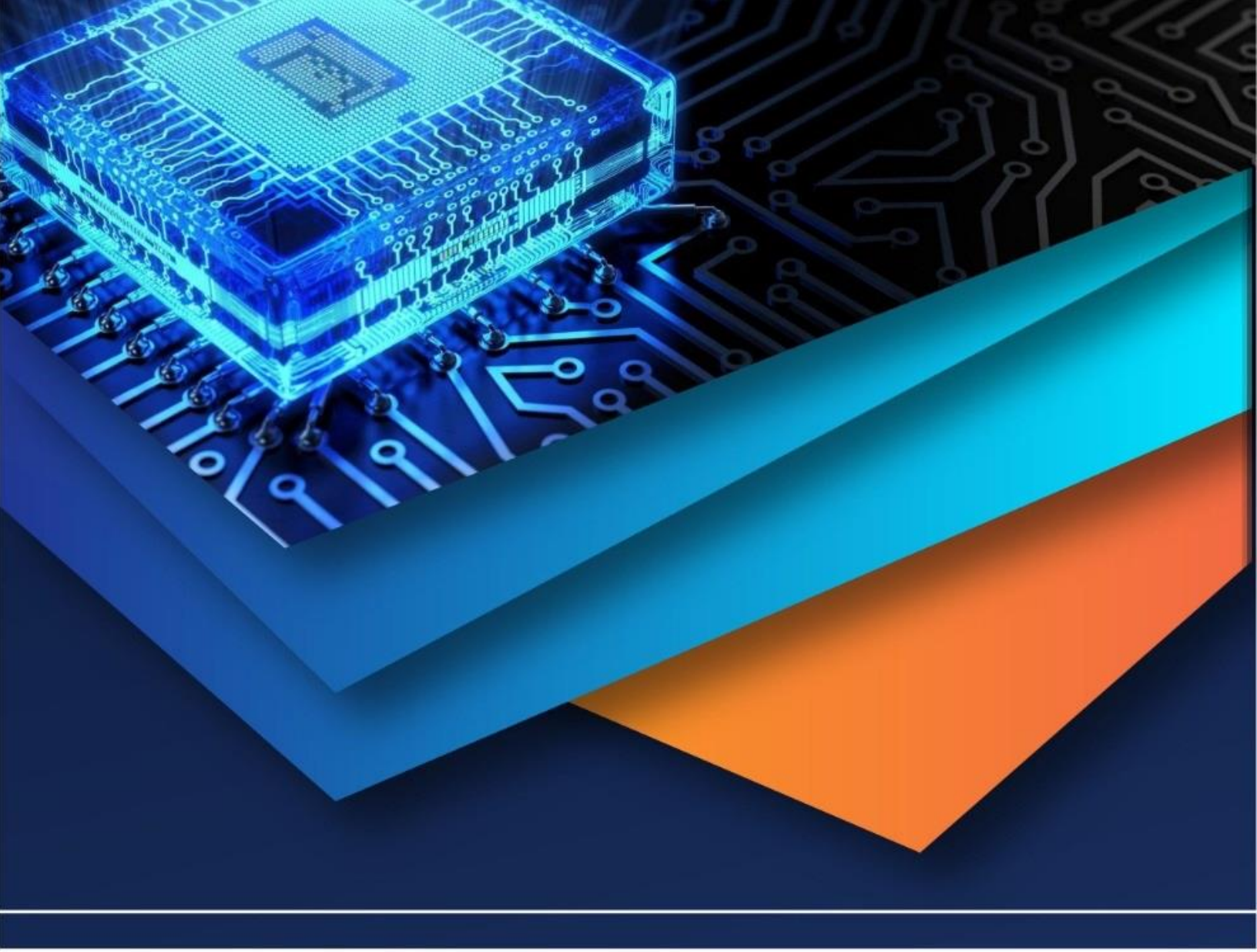

10.22214/IJRASET

45.98

IMPACT FACTOR: 7.129

IMPACT FACTOR: 7.429

INTERNATIONAL JOURNAL FOR RESEARCH

IN APPLIED SCIENCE & ENGINEERING TECHNOLOGY